ent feedback mechanisms were at work. Scientists are working to determine if the SST–flux relationship in the Pacific suggests a response of the atmosphere to the oceanic forcing, and if the SST–flux relationship in the Indian Ocean implies an atmospheric forcing for the ocean.

Outside of the Tropics, the influence of eddy-scale structures is evident in the 2-yr difference map. Nevertheless, the difference anomalies are most pronounced in the vicinity of the two WBCs, that is, the Kuroshio and the Gulf Stream, and their extensions. For the former, there were negative LHF + SHF anomalies over almost the entire region; while for the latter, there were negative flux anomalies south of the Gulf Stream extension and positive anomalies north of the current. A colder sea surface coupled to slightly weakened wind speed appears to be the cause of the reduced LHF + SHF in these regions. It may be worth noting that the SSTs in the Kuroshio and its extension are generally lower than normal during the ENSO warm phases (White and He 1986). The connection between lower SST and less oceanic heat loss is another indication of the response of the atmosphere to oceanic forcing.

The long-term context of the change in ocean heat fluxes in 2006 is shown in the plot of year-to-year variations of the globally averaged annual mean from 1958 to 2006 (Fig. 3.6). The 2006 mean of LHF + SHF was at a similar level to the 2005 mean. However, the two recent years are located at the high end of a long-term upward trend that started in 1977/78. Since then, LHF + SHF have increased by about 9 W m^{-2}, from a minimum at ~99 W m^{-2} in 1977 to a maximum at ~108 W m^{-2} in 2003. The magnitude of the variability is dominated primarily by LHF. SHF is about one order smaller than LHF, and the change in SHF is also small (less than 2 W m^{-2} over the entire 50-year analysis period). Nonetheless, the trend in SHF is very different from that in LHF: the downward trend in SHF lasted until the late 1980s, followed by a few abrupt jumps in the early 1990s. Since 2000, SHF has tended downward.

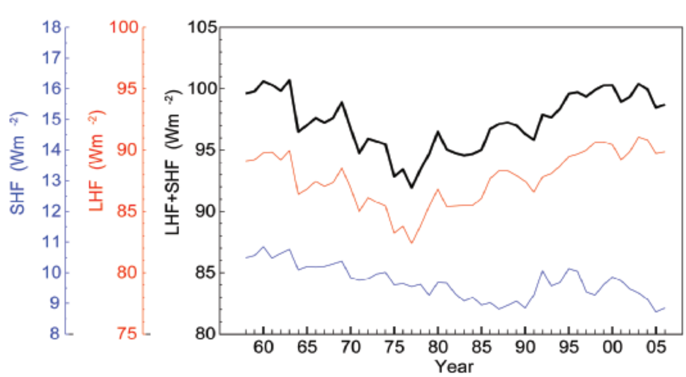

Fig. 3.6. Year-to-year variations of globally averaged annual mean latent plus sensible heat flux (black), latent heat flux (red), and sensible heat flux (blue).

c. *Sea surface salinity*—G. C. Johnson and J. M. Lyman

Ocean storage and transport of freshwater are intrinsic to many aspects of climate, including the global water cycle (e.g., Wijffels et al. 1992), El Niño (e.g., Maes et al. 2006), and global climate change (e.g., Held and Soden 2006). Regional studies of decadal freshwater variability are possible in well-sampled regions like the North Atlantic (e.g., Curry and Mauritzen 2005). In addition, zonal averages of long-term global trends of salinity in each ocean basin have been analyzed (Boyer et al. 2005). In situ ocean salinity data have traditionally been too sparse and their reporting too delayed for an annual global perspective of ocean freshwater and its complement, salinity. However, the rapidly maturing Argo array of profiling floats (Roemmich et al. 2004) is remedying this situation. Argo data are used here to present annual average SSS analyses for 2006 and 2005, the first years with near-global Argo coverage. Remote sensing of SSS by satellite is planned for 2009 (information online at http://aquarius.nasa.gov/).

Here the shallowest near-surface (< 25 m) salinity data flagged as good from each available Argo profile for the years in question were subjected to a statistical check to discard outliers. The remaining data were then cast as differences from a climatological mean surface salinity field from the WOA based on historical data reported through 2001 (WOA 2001; Boyer et al. 2002). The resulting anomalies were then mapped, essentially assuming a Gaussian covariance function with 6° latitude and longitude decorrelation length scales and a signal-to-noise variance ratio of 2.2 (Bretherton et al. 1976).[1]

SSS patterns are fairly well correlated with surface freshwater flux, the sum of evaporation, precipitation, and river runoff (e.g., Behringer et al. 1998). In each ocean basin, subtropical salinity maxima centered near 20° or 25° in latitude are signatures of the predominance of

[1] While some delayed-mode scientific controlled (final) Argo data are available for the 2005/06 time period, many real-time (preliminary) Argo data were used in both years. The real-time estimates of SSS made here could change after all the data have been subject to careful scientific quality control.

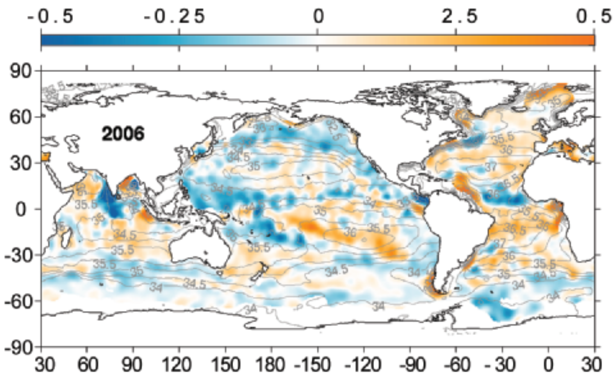

Fig. 3.7. Map of the 2006 annual surface salinity anomaly estimated from Argo data (colors in PSS-78) with respect to a climatological salinity field from WOA 2001 (gray contours at 0.5 PSS-78 intervals). White areas are either neutral with respect to salinity anomaly or are too data poor to map. While salinity is often reported in practical salinity units it is actually a dimensionless quantity reported on the PSS-78.

evaporation over precipitation. Conversely, in most regions where climatological surface salinities are relatively fresh, precipitation generally dominates over evaporation. The 2006 anomalies from WOA 2001 (Fig. 3.7) reveal some large-scale patterns. In 2006 the regions around the climatological salinity maxima are mostly salty with respect to WOA 2001. In many of the climatologically fresh regions, 2006 values appear fresher than those of WOA 2001, including most of the ACC near 50°S, the subpolar gyre of the North Pacific, and the ITCZ over the Atlantic and Pacific Oceans (including the SPCZ).

These patterns may suggest an increase in the hydrological cycle (more evaporation in drier locations, and more precipitation in rainy areas), as depicted in simulations of global warming. These simulations do suggest that this signal might be discernible during the last two decades of the twentieth century (Held and Soden 2006). Any increase in the hydrological cycle would certainly result in changes of local SSS values, but not alter the global average salinity by itself. Most of these patterns observed in 2006 (Fig. 3.7) are not reflected in the 2005–06 differences (Fig. 3.8), suggesting that these anomalies have evolved over longer-than-interannual time scales; although, without global coverage prior to 2005, it is difficult to determine the time scale. However, there are alternate explanations. It is possible that the climatology, being based on relatively sparse data distributions in many parts of the oceans, may tend to underestimate regional extrema that the well-sampled Argo array can better resolve. Also, some of these patterns might be explained by interannual shifts in ocean features such as the ACC or atmospheric features such as the ITCZ.

For example, the subpolar North Atlantic and Nordic Seas are relatively salty, both in 2006 (Fig. 3.7) and in 2005 (not shown), with relatively small changes between these two years (Fig. 3.8). This salty anomaly is inconsistent with an increase in the strength of the hydrological cycle. However, the pattern may have less to do with local evaporation and precipitation fields and more with northward spread of saltier waters from the south. The salty anomaly in this region is consistent with a stronger influence of subtropical gyre waters in the northeastern North Atlantic in recent years and a reduced extent for the subpolar gyre (Hátún et al. 2005).

There are evidently some rather large anomalies in the equatorial and North Indian Ocean. The Bay of Bengal and much of the Arabian Sea appear to be anomalously salty, while the ocean to the south and east of India appears to be fresh (Fig. 3.7). The changes appear to be interannual, as reflected in the large changes in anomaly between 2005 and 2006 in this region (Fig. 3.8).

One last feature of interest in the 2006 salinity field is the anomalously salty water located in the region of the fresh Amazon River plume (Fig. 3.7). The influence of this plume would normally be apparent in the relatively fresh conditions to the north and west of the mouth of the Amazon River (near the equator) that reach as far north as Puerto Rico. The salty anomaly in this region in 2006 may be explained by the reduced freshwater flow from the Amazon into the ocean during a record drought in the Amazon River basin in 2005 (Shein et al. 2006), with some time delay for hydrological and oceanic processes. The change in salinity between 2005 and 2006 (Fig. 3.8) shows that this salty anomaly is limited to 2006.

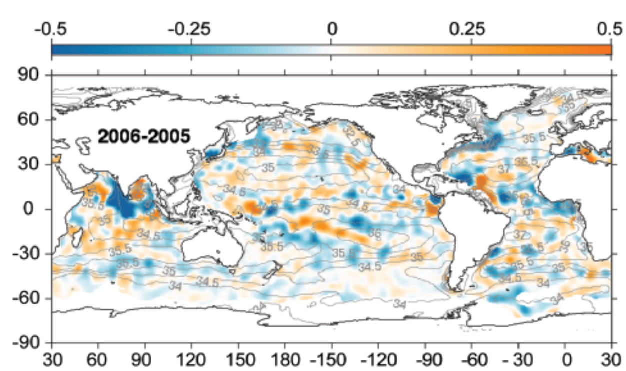

Fig. 3.8. The difference of 2006 and 2005 surface salinity maps estimated from Argo data (colors in PSS-78 yr^{-1}). Other details follow Fig. 3.7.